ADVANCED FUNCTIONAL MATERIALS
www.afm-journal.de

Nanofiltration Membranes with Modified Active Layer Using Aromatic Polyamide Dendrimers

Yuan Gao, Ana M. Saenz de Jubera, Benito J. Mariñas, and Jeffrey S. Moore**

The modification of a commercial nanofiltration (NF) membrane (TFC-S) with shape-persistent dendritic molecules is reported. Amphiphilic aromatic polyamide dendrimers (G1–G3) are synthesized via a divergent approach and used for membrane active layer modification by direct percolation. The permeate samples collected from the percolation experiments are analyzed by UV-visible spectroscopy to monitor the influence of dendrimer generations on percolation behavior and active layer modification. Further characterization of modified membranes by Rutherford backscattering spectrometry and atomic force microscopy techniques reveals a relatively low-level accumulation of dendrimers inside the original TFC-S NF membrane active layer and subsequent formation of a coating of pure aramide dendrimers on top of the active layer. A PES-PVA ultrafiltration membrane is used as a control membrane support (without an NF active layer) showing that structural compatibility between the dendrimers and support plays an important role in the membrane modification process. The performance of the modified TFC-S membrane is evaluated on the basis of the rejection abilities for a variety of water contaminants having a range of molecular size and chemistry. As the water flux is inversely proportional to the thickness of the active layer, the amount of dendrimers deposited for specific contaminants are optimized to improve the solute rejection while maintaining high water flux.

1. Introduction

One of the most severe problems worldwide is inadequate access to sufficient clean water, which motivates research on new materials for water purification and reuse.[1] In the last decade, nanofiltration (NF) has emerged as an efficient and economical drinking water treatment process, because of its ability to remove various contaminants from water in a single treatment step with low operating pressure (typically 0.3–3 MPa) and relatively high solute rejection as well as high water permeation.[2] Commercially-available NF membranes are typically a composite structure with a ca. 50 μm asymmetric porous support layer and a ca. 100–200-nm-thin active layer; the latter serves as a barrier to water contaminants.[3] The active layers are usually made by the method of interfacial polymerization resulting in a thin film of crosslinked polyamide with incompletely crosslinked carboxylic groups providing a negative charge.[4] Most commercial membranes face similar challenges such as a propensity to undergo fouling[5] and inability to adequately reject certain common water contaminants, e.g., arsenic(III), predominantly in the form of arsenious acid (H_3AsO_3) in natural waters.[6] Therefore, there is a need to develop a new generation of NF membranes having active layers with adjustable chemistry and structure to achieve fouling resistance and desired water/solute selectivity for the broad range of conditions encountered in water quality control applications.

Many approaches to improve commercial NF membrane performance have been tried, including coating, plasma treatment, chemical treatment, grafting polymerization, and UV irradiation.[7] The resulting membranes have generally demonstrated increased hydrophilicity as well as improved water permeability and antifouling ability.[8] However, decreased salt rejection was observed for certain modified polyamide membranes.[8b] Furthermore, increased contaminant rejection is usually accompanied with significant decrease in water flux.[9]

A versatile approach to membrane modification that utilizes well-defined macromolecular architectures was described recently.[10] In that study, shape-persistent macromolecules are synthesized and directly percolated through a support film to fabricate a new generation of NF membranes. Rigid star amphiphiles (RSAs) with 1–2 nm hydrophobic cores and hydrophilic side chains were coated onto polyethersulfone (PES) ultrafiltration (UF) membrane supports to create NF membranes.[10] Characterization of these membranes revealed that the RSAs produced a uniform active layer atop the PES support, but also that some of the macromolecules penetrated deeper into the support, blocking pores and reducing the water flux.

Y. Gao, Prof. J. S. Moore
Departments of Chemistry and Materials Science and Engineering and Center of Advanced Materials for the Purification of Water with Systems
University of Illinois at Urbana-Champaign
Urbana, IL 61801, USA
E-mail: jsmoore@illinois.edu
A. M. S. de Jubera, Prof. B. J. Mariñas
Department of Civil and Environmental Engineering and Center of Advanced Materials for the Purification of Water with Systems
University of Illinois at Urbana-Champaign
Urbana, IL 61801, USA
E-mail: marinas@illinois.edu

DOI: 10.1002/adfm.201201004

The rejection of arsenic(III) achieved with the RSA membranes was comparable to the rejection obtained by the commercial NF membranes ESNA and TFC-S.[11] These findings encourage us to extend this molecular deposition method to the modification of commercial polyamide NF membranes. The small pore size distribution of NF membranes prevents building block molecules from breaking through, thus minimizing internal pore blocking and associated water flux decrease as a result of membrane modification.[12] Here, we survey the use of aromatic polyamide dendrimers with varied compositions and structures for membrane modification.

Dendrimers are regularly branched, three dimensional macromolecules. Many of their characteristics, for example the size and shape of the molecule and the position of functional groups, can be well controlled by systematic changes in their synthesis. Thus, they are designed to exhibit unique properties, such as good solubility, low viscosity, multivalence, and encapsulation effects, leading to a variety of applications.[13] In recent years, aromatic polyamide (aramide) dendrimers have been prepared by both convergent and divergent synthetic approaches.[14] They maintain the good thermal, chemical, and mechanical properties of linear aromatic polyamides, but with improved solubility, functionality, and processability. From a structural point of view, there is high similarity between these aramide dendrimers and the interfacial polymerized polyamides in NF membrane active layers, which provides similar chemical properties and strong interactions between aramide dendrimers and membrane active layers, making them good candidates for polyamide NF membrane modification. Moreover, unlike the highly crosslinked and cyclized polyamides in active layers, aramide dendrimers have sufficient solubility in organic solvents. Therefore, they have the potential to be deposited on the support membrane by percolation. By increasing the dendrimer generation and tailoring the peripheral group chemistry, it is possible to use these structurally well-defined aramide dendrimers to systematically investigate membrane-performance relationships.

This article describes the synthesis and characterization of amphiphilic aramide dendrimers with well-defined branched structures for the modification of polyamide active layers of NF membranes by direct percolation onto the support. A series of bidendron aramide dendrimers were chosen as target compounds (**Figure 1**).[15] Since the repeating unit has all substitutes in the *m*-position, the aramide dendrimers are good mimics to the polyamide networks used in commercial membranes, but with a perfectly defined molecular structure. *p*-Phenylenediamine (PDA) as the core structural unit reduces the steric hindrance between the two dendritic segments. Oligoethylene glycol (OEG) side chains were attached to the dendrimer's periphery through amide bond linkages[16] for the dual purpose of overcoming the dendrimer's limited solubility in methanol and providing greater hydrophilicity for membrane fouling resistance. These dendrimers were then deposited onto a commercial polyamide NF membrane (FLUID SYSTEMS TFC-S, Koch Membrane Systems, Wilmington, Massachusetts) for membrane modification. In addition, similar procedures were performed with PES membranes as a support layer (without active layer) control experiment. The quality of the aramide dendrimer modified active layers was characterized by UV-vis spectroscopy, atomic force microscopy (AFM) and Rutherford backscattering spectrometry (RBS). Membrane performance was evaluated on the basis of rejection capabilities of organic contaminant surrogate Rhodamine WT (R-WT), and sodium chloride, barium chloride and arsenic(III).

2. Results and Discussion

2.1. Synthesis and Characterization of Aramide Dendrimers

The synthesis of aramide dendrimers G1–G3 followed a facile divergent approach recently reported by Ueda and coworkers (**Scheme 1**).[15] Amine-terminated NH_2-Gn (n = 1–3) were synthesized by using 3,5-bis(trifluoroacetamido)benzoyl chloride as an AB_2 building block with all reactions carried out in a single flask. 2-[2-(2-Methoxyethoxy)ethoxy]acetyl chloride, which was

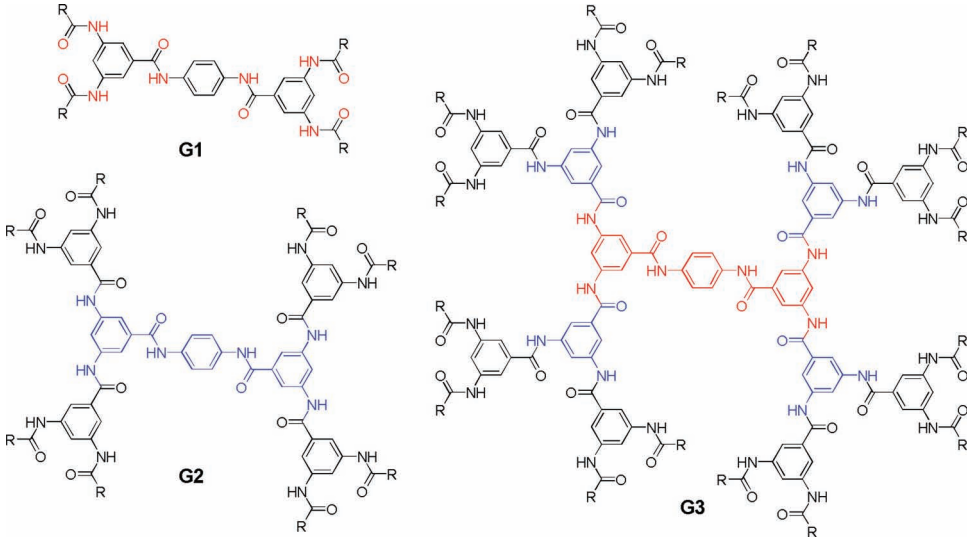

Figure 1. Aramide dendrimers with an OEG periphery (G1–G3); R = -$CH_2O(CH_2CH_2O)_2CH_3$.

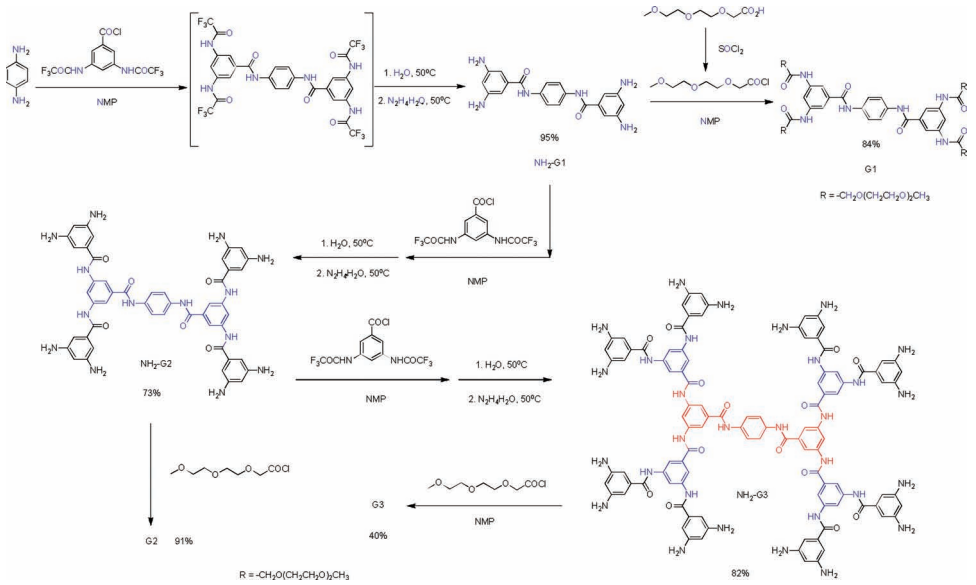

Scheme 1. Synthesis of aramide dendrimers with an OEG periphery (G1–G3).

obtained by reacting 2-[2-(2-methoxyethoxy)ethoxy]acetic acid with thionyl chloride, was used to functionalize the amine-terminated NH_2-Gn (n = 1–3) by amide bond formation.[17] Aramide dendrimers G1–G3 were then obtained in moderate yield after column chromatography.

The structures of dendrimers G1–G3 have been characterized by ^{1}H NMR, ^{13}C NMR, MALDI-TOF mass spectrometry and gel permeation chromatography (GPC). The ^{1}H NMR spectrum of the dendrimers showed signals in three chemical shift regions corresponding to amide, aromatic, and ethylene glycol side chain protons. As shown in **Figure 2**, the MALDI-TOF mass spectra of dendrimers G1–G3 gave m/z values of 1039.0, 2215.8, and 4567.5 Da, which are within experimental error of their calculated m/z values of 1039.5, 2215.9, and 4568.9 Da, respectively. Furthermore, the GPC traces of all three dendrimers were unimodal and had narrow distributions (**Figure 3**). These results confirmed the formation of the desired dendrimers.

In order to quantify the amount of polyamide dendrimers within a molecular thin film (i.e., using the Rutherford backscattering spectrometry technique), heavy elements, such as iodine, are incorporated into dendrimer molecules.[10] Due to the divergent feature of the approach, the synthesis is facilitated by incorporating iodine atoms into the dendrimer core. Thus, 2,6-diiodobenzene-1,4-diamine was synthesized by reduction of diiodonitroaniline and used for dendrimer preparation in the same way as for dendrimers G1–G3.[18] Dendrimers 2I-Gn (n = 1–3) were obtained in the yields of 43, 72, and 56%, respectively. Their structures have been characterized by ^{1}H NMR, ^{13}C NMR, and MALDI-TOF mass spectrometry. The ^{1}H NMR spectrum of dendrimer 2I-G1 showed peaks corresponding to the amide protons at chemical shifts of 10.46, 10.28, and 9.87 ppm, and peaks corresponding to the aromatic protons at 8.38, 8.25, 7.90, and 7.84 ppm, indicating the asymmetric nature of the diiodo-substituted compounds. The MALDI-TOF mass spectra showed signals corresponding to the dendrimer molecular weight peaks with m/z values at 1271.0, 2467.1, and 4818.9 Da, while the calculated m/z values are 1268.9, 2467.7, and 4820.7 Da, respectively. According the ^{1}H NMR spectra, the purity of these dendrimers is over 95%, as no signals from byproducts were observed.

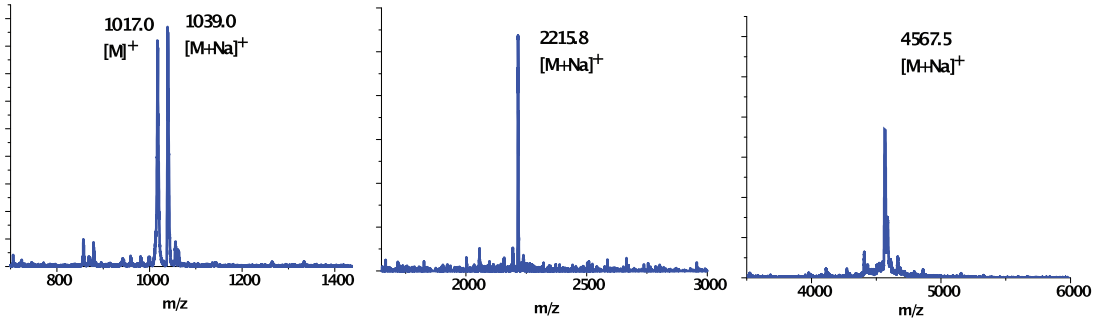

Figure 2. MALDI-TOF MS spectrum of aramide dendrimers G1–G3.

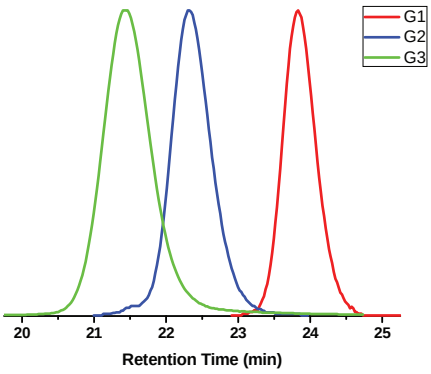

	M_n	M_w/M_n
G1	1800	1.03
G2	4000	1.03
G3	6200	1.03

Figure 3. GPC traces of aramide dendrimers G1–G3.

2.2. Percolation of Aramide Dendrimers with the PES UF Support

For the control experiments, aramide dendrimers G1–G3 were deposited on a previously described polyvinyl alcohol (PVA) modified PES UF membrane by percolation.[10] The PVA was used to plug the largest pores of the support for the purpose of lowering advective permeation. With such support membranes, we are able to compare the effect of aramide dendrimers with our previous results with RSAs and to survey the influence of dendrimer size on the interaction between dendrimers and support membranes.

Dendrimers G1–G3 were dissolved in methanol at approximately 6 mg/L, and percolated through the above support film. Percolated samples were collected as a function of time, and the product flux of methanol (**Figure 4**a) was measured gravimetrically with an analytical balance connected to a computer.[10] In the blank experiment with pure methanol solvent, an approximately constant flow rate was maintained over the whole percolation time. In contrast, all of the aramide dendrimer solutions underwent a decrease in percolation flow to various degrees. Dendrimer G1 had the smallest effect on the percolation flow, with the flow rate decreasing to about 67% of the initial value. On the other hand, both dendrimers G2 and G3 caused more significant reduction in the percolation flow, leading to only 20% and 28% of the initial value, respectively. These flow rate changes are consistent with G1 having less interaction with the membrane meaning that it likely gets washed through the support. In contrast, G2 and G3 resulted in greater permeate flux resistance, consistent with higher pore blockage of the support.[19] Though the pore size of the PES support is not known, the molecular weight cut-off reported by the manufacturer is in the range of 0.9 to 2.3 kDa.

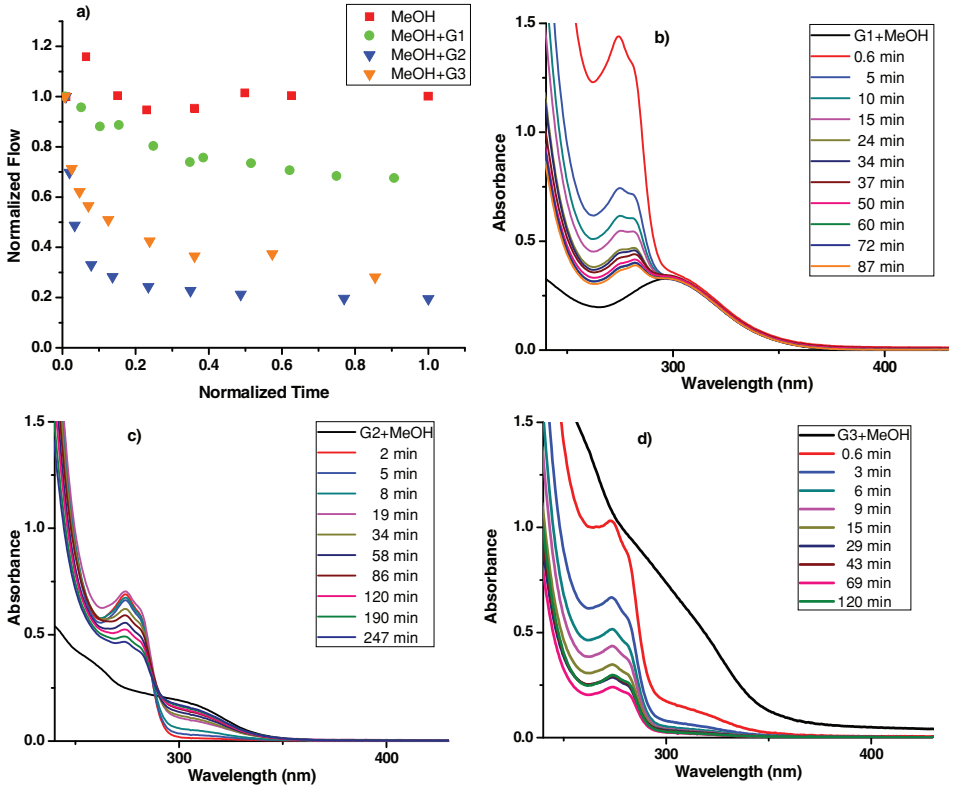

Figure 4. a) Permeate flow of various dendrimer solutions in methanol and a methanol blank as a function of sampling time for the modified PES-PVA membranes. b), c) and d) are the UV-vis spectra of permeate versus time for G1, G2, and G3 dendrimer solutions, respectively. The presence of the dendrimers in the permeate solutions is evident by absorption in the wavelength range of 295 to 350 nm. The lines labeled as G_i+MeOH in the legends indicate the feed solutions of the dendrimers in methanol.

We believe that G2 could impact more the membrane flow rate compared to G3 since the molecular weight of G2 is in the range of the PES cut-off, closer to the upper limit, and it could therefore cause more pore blockage.[19]

The permeate samples collected from the percolation experiments were analyzed by UV-vis spectroscopy to provide direct information about the amount of dendrimers in the permeate solutions as a function of the percolation time (Figure 4b–d). For dendrimer G1, the UV-vis spectra for all samples, including feed solution and permeates, showed the same absorption intensity at 300 nm, the band associated with the π–π^* transition of the aramide dendrimers.[20] These observations indicate that G1 broke through the support at a constant rate with little retention. In contrast, the absorption intensity for dendrimer G2 at 300 nm continuously increased over time until reaching a value close to that of the feed solution. Thus, dendrimer G2, which diffused into the support membrane pores, blocked small pores, slowly permeated through large pores of the support film with the passage of time, and eventually fully broke through. Finally, the absorption spectra for G3 showed intensity at 300 nm decreasing to a value close to zero. This observation suggested that most G3 dendrimers stayed within or on top of the support film after the initial penetration by a small fraction of G3s. The decreasing concentration of dendrimer G3 in the permeate with filtration time, indicates that initially, G3 blocks some pores or imperfections in the PES-PVA support, and this apparently obstructs subsequent G3s from breaking through those pores. However, the location of the G3 molecules, whether they were on top of the PES-PVA or inside it, can not be obtained from the UV-vis results. These findings show the importance of dendrimer size on membrane modification and they are consistent with the trends observed for methanol permeation (Figure 4a).

In order to identify the spatial distribution of aramide dendrimers on and within the PES-PVA support, RBS experiments were carried out to provide a depth profile of the elemental concentration using methods similar to those previously reported for RSA membranes.[10] Following similar procedures to those used to prepare the membranes with G1–G3, target membranes were prepared with aramide dendrimers of three generations, each of which contained two iodo groups (2I-G1, 2I-G2, and 2I-G3). Approximately one mg of the dendrimer molecules was applied to the supports during the percolation. The amount of retained aramide dendrimers on PES-PVA membranes varied with dendrimer generations similar to the non-iodinated dendrimers noted above. Once the filtration was finished, the membrane coupons were air dried and subjected to RBS analysis, in which a 2-MeV He^+ beam was directed onto the membrane surfaces with the backscattering particles providing information on elemental composition as a function of sample depth.

Figure 5 shows a comparison of membranes fabricated with the three dendrimer generations on the PES-PVA support. The iodine signals are identified as diagnostic peaks for the presence of iodinated aramide dendrimers on the membrane. The position and intensity of these peaks provide direct information on the location of the dendrimers. In all three cases, the dendrimer molecules impregnated the PES-PVA support, with little or no dendrimers on top. The broad

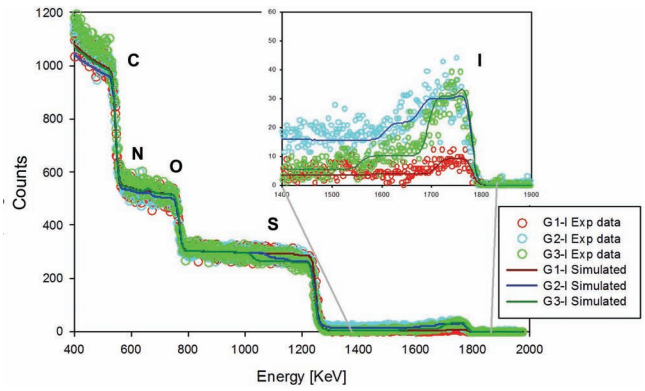

Figure 5. RBS spectra of the PES-PVA membranes that have been modified with iodinated aramide dendrimers. The simulation of experimental data was performed with the program SIMNRA.[21]

plateaus at ca. 1550–1800 keV, are consistent with a wide distribution of dendrimer molecules inside the support. A mass balance simulation was performed to the RBS spectrum of the iodinated dendrimer modified membrane using the computer program SIMNRA.[21] For the case of the 2I-G3 dendrimers, the iodine peak at ca. 1780 keV suggested that a small amount (on average less than 1%) of the macromolecules stayed on top of the PES-PVA support forming a discontinuous coverage, while the majority of the 2I-G3 dendrimers were found inside the PES-PVA support at the highest concentration close to the surface. The 2I-G2 dendrimers were found inside the PES-PVA membrane at higher concentrations than the 2I-G3s with a barely detectable amount on top. The mass balance and RBS spectrum for 2I-G1 showed that G1 could also be found inside the PES-PVA, but at much lower concentrations than the other two larger dendrimers, since as the UV-vis data showed almost all G1 dendrimers were recovered in the permeate.

The solute rejection performance of the new generated membranes was studied using R-WT as a surrogate for trace organic contaminants.[10] Fluorescence analysis indicated R-WT rejection was constant at approximately 80%, similar to the PES-PVA blanks, and much lower than that of 98–99% for a RSA deposited PES-PVA membrane, for the feed pressure range tested of 0.21 to 0.41 MPa (data not shown).[11] The formation of a dense dendrimer layer on top of the PES-PVA support would have increased the rejection data to values closer to those obtained with the RSA molecules. Therefore, R-WT rejection experiments validated the RBS findings of the lack of formation of a thick dendrimer layer on top of the PES-PVA membrane.

The above findings were compared with the previous results on RSAs deposited PES-PVA membranes to obtain further understanding of the interactions between dendrimers and support membranes.[10,11] The RBS spectra for all three dendrimer deposited membranes are similar to those RSA membranes of high water permeability, whereby RSAs only adsorbed inside the support without forming a detectable thin layer of pure RSA.[10] Such high water permeability (A_D = 5.2 m/(MPa·d)) was comparable to that of the G3 membrane and slightly larger than that of the G2 membrane (Supporting

Information).[11] However, continuing percolation did not result in the formation of a thick dendrimer layer onto the support which was observed for RSAs. The possible reason for such difference is that the aramide cores of the dendrimers are more hydrophilic than the hydrophobic oligophenylene cores of the RSAs. At this point we reasoned that the high hydrophilicity of the aramide dendrimers could be more advantageous for the modification of commercial polyamide NF membranes. As the pore size distribution is smaller for the NF membranes, the aramide dendrimers can still be stabilized with a low hydrophobic interaction. The relatively high hydrophilicity might help maintain good water flux and also improve rejection to potential hydrophilic contaminants.

2.3. Percolation of Aramide Dendrimers with the TFC-S NF Membrane

The TFC-S membrane was chosen as representative of commercial polyamide NF membrane for the dendrimer modification.[22] Compared to other commercial membranes, TFC-S exhibits relatively low rejection performance for salts, arsenious acid, and organic molecules.[10,23] Improvement in contaminant rejection by the dendrimer modification could thus be discernible. Unlike the PES support, PVA modification was not necessary in case of the TFC-S membrane, thus, simplifying the membrane preparation process.

The modification for the TFC-S NF support was performed in a similar manner as for the control PES-PVA UF support, in which the membrane was loaded with approximately one mg of the dendrimer. Permeate was collected as a function of time, and the flux of the methanol was measured gravimetrically (**Figure 6**a). Dendrimer G1 caused a decrease in the percolation flow to about 76% of the initial value, while dendrimers G2 and G3 caused higher flux decreases, as to 30% and 59% of the initial flux, respectively. In each case, the percent decrease in methanol permeate flow was smaller for the TFC-S membrane than for the PES-PVA membrane. The result was consistent with the high ratio of macromolecule size to pore size for the TFC-S membrane, which can be as high as 13 when the G3 is compared to the TFC-S smallest pores and 3.5 when G3 is compared to the TFC-S largest pores, favoring a lower level of pore blockage and a smaller flux drop. UV absorption measurement showed that dendrimer G3 did not break through the TFC-S membrane after the initial stage of the percolation period (Figure 6d). In contrast both G1 and G2 broke through, although the quantity of G2 was less than that of G1 (Figure 6b,c). Since the absorbance intensity for permeate samples never reached the level observed for feed solutions in all three cases, it is expected that aramide dendrimer molecules

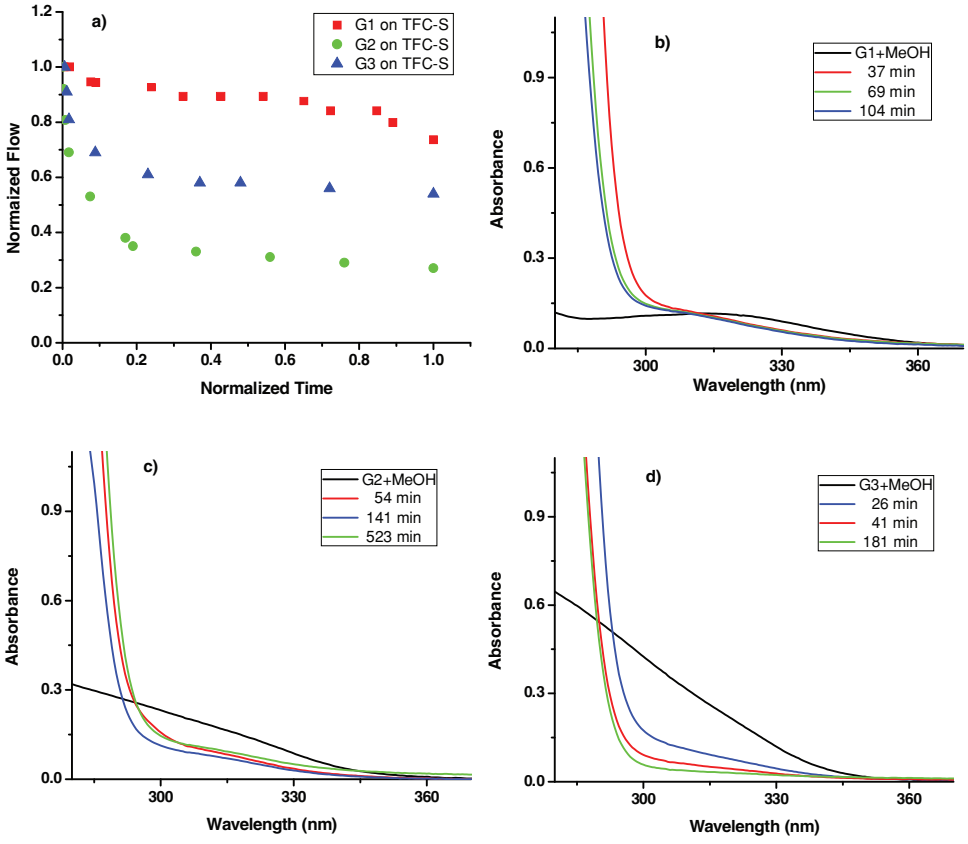

Figure 6. a) Permeate flow of various dendrimer solutions in methanol versus sampling time for the TFC-S NF membranes. b), c) and d) are UV-vis spectra of permeate as a function of time for G1, G2, and G3 dendrimer solutions respectively. The presence of the dendrimers in the permeate solutions is evident by absorption in the wavelength range of 295 to 350 nm. The lines labeled as Gn+MeOH in the legends indicate the feed solutions of the dendrimers in methanol.

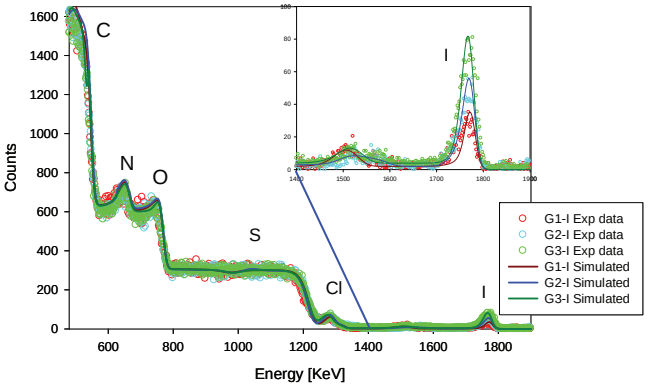

Figure 7. RBS spectra of the TFC-S membranes that have been modified with iodinated aramide dendrimers. The simulation of the experimental data was performed with the program SIMNRA.[21]

accumulated and a thin layer built up on top of the TFC-S membranes. Evidence of this behavior was obtained by RBS measurements using iodo-labeled dendrimers.

The RBS spectra of iodinated aramide dendrimers (2I-Gn, n = 1–3) modified TFC-S membranes are shown in **Figure 7**. For all three dendrimer generations, the relatively narrow and isolated iodine peaks at ca. 1750–1800 keV indicate that the iodinated dendrimers had a narrow spatial distribution along the membrane.[10] SIMNRA was used to fit the experimental spectra in order to simulate the location of iodine atoms contained in dendrimers.[21] For all three dendrimers, the best fit for these iodine peaks was obtained by assuming that the dendrimers filled ridge-and-valley of the TFC-S polyamide active layer, and further formed a layer on top of the original active layer.

The average thickness of the dendrimer layer atop the polyamide was calculated with the expression reported by Mi et al.[3] Considering a commercial polyamide has a density ranged between 1.09 and 1.24 g/cm^3, the density of the aramide dendrimers was assumed to have an average value of 1.1 g/cm^3, due to the structural similarity between dendrimers and such linear polymers.[24] Increased thickness was observed for the dendrimer layer with higher generation. The fit for the iodine peaks in the range 1750–1800 keV revealed that the dendrimers' layer thickness was around 14 nm for G1, 25 nm for G2, and 41 nm for G3. These findings indicate that larger dendrimer molecules accumulated more effectively on the TFC-S membranes, thus forming thicker layers.

The aramide dendrimers that broke through the membrane absorbed preferentially in a defined region of the support, as shown by the broad RBS peaks between 1400 and 1600 keV. The low peak intensity suggested that the amount of those dendrimer molecules was relatively small. The occurrence of a gap between the top layer of pure dendrimer and the layer of dendrimer absorbed inside the support was also observed by Lu et al. for the RSA membranes.[10] In the case of the RSA, RBS data were best modeled as having a thin vacant layer next to the support interface with a thickness of approximately 40 nm and RSAs being absorbed in subsequent sublayers each with a thickness of about 185 nm at a constant concentration within each sublayer. However, the separation between the dendrimer top layer peak (ca. 1750–1800 keV) and the membrane-adsorbed dendrimer peak (ca. 1400–1600 keV) was more pronounced for the dendrimer modified TFC-S membranes. Furthermore, instead of forming subsequent sublayers, the single peak between 1400 and 1600 keV revealed that only one sublayer existed in the PS support. The three RBS spectra are thus analyzed as low-level accumulation of dendrimers inside the TFC-S NF membranes and subsequent formation of an additional layer of pure aramide dendrimer on top of the original active layer.

The dendrimer-modified TFC-S membranes were further characterized by AFM to study the surface morphology and roughness.[25] Generally, the surface roughness increased with the dendrimer generation. The roughness change was especially prevalent from the membrane with dendrimer G1 layer to the one with G2 layer. There were more irregularities and protuberances on the membrane surface with G2 or G3 active layer than other ones (see Supporting Information for representative AFM images). A more accurate evaluation of the surface roughness is provided by the root-mean-square (RMS) roughness, which was obtained by scanning an area of 10 μm × 10 μm by AFM in tapping mode (**Table 1**). The RMS roughness for the commercial TFC-S membrane was 25.9 nm, and it increased to 32.0 nm for G1-modified membrane. The values increased significantly for the membranes modified with G2 and G3, being measured as 41.3 and 44.4 nm, respectively. The AFM analysis revealed an uneven distribution of dendrimers in the top layer, probably due to molecular agglomeration in areas of higher permeability on the TFC-S membrane surface.

The performance of the modified TFC-S membranes was evaluated by measuring their transport properties including water flux and rejection of arsenious acid, a representative small, neutral contaminant (full details are reported elsewhere[26]). It was found that dendrimer G1 modified membrane was not stable during the rejection test, as small size G1 broke though the pores of the NF active layer. However, for both G2 and G3 modified membranes, significantly increased rejection to arsenic(III) was measured. Rejection up to 70% was observed compared to the original membrane rejection of ca. 20%. Considering that only 1 mg of dendrimer molecules was deposited on a 14 cm^2 membrane coupon, the areal density of dendrimer loaded on the TFC-S membrane samples could be estimated as 71 μg/cm^2 assuming uniform coverage. Although a significant improvement in rejection performance was observed for dendrimer-modified membranes, the water flux dropped 80%

Table 1. Root-mean-square roughness values obtained from AFM measurements[a)] for unmodified and aramide dendrimer-modified (71 to 3.6 μg/cm^2) TFC-S membranes.

Membrane	RMS Roughness [nm]
Unmodified TFC-S	25.9 ± 1.0
TFC-S modified with 1mg G1	32.0 ± 1.1
TFC-S modified with 1mg G2	41.3 ± 2.0
TFC-S modified with 1mg G3	44.4 ± 1.8
TFC-S modified with 0.05 mg G2	31.1 ± 4.8
TFC-S modified with 0.05 mg G3	34.0 ± 1.6

[a)]Representative AFM images are shown in the Supporting Information.

from that of the original TFC-S membrane. Because the water flux is inversely proportional to the thickness of the active layer, we optimized the amount of dendrimers deposited for specific contaminants to improve the solute rejection while maintaining high water flux.

In a systematic study, dendrimers G2 and G3 with amounts 0.1, 0.05, 0.03, and 0.01 mg were deposited on the TFC-S membrane by percolation, respectively.[26] The areal densities of dendrimer loaded on TFC-S membrane were then estimated as 7.1, 3.6, 2.1, and 0.71, respectively. AFM images were collected for the TFC-S membranes modified with 0.05 mg dendrimers of these two generations (Supporting Information). The RMS roughness for these membranes was measured as 31.1 and 34.0 nm, respectively (Table 1). These values were slightly higher than that of the original membrane and relatively close to the value of the membrane modified with one mg of G1. Such a result suggested that the small amount of dendrimer deposited mainly filled the ridge-and-valley of the TFC-S polyamide active layer, which was consistent with RBS measurements (Supporting Information).

Figure 8 shows the rejection of modified TFC-S membranes for prototypical water contaminants. Membrane performance was measured for each of the solutes with the TFC-S membrane without modification (blank sample) and for the same NF membrane modified with different amounts and different types of dendrimers.[26] In order to compare the membrane rejection between various contaminants, all data were acquired with a permeate flux of 0.4 m/day. As for R-WT, even 0.71 μg/cm^2 dendrimer loading on the TFC-S membrane increased the rejection from ca. 98.3% to over 99.4%, which means the contaminant concentration in the permeate was almost one order of magnitude lower than for the unmodified membranes. Specifically, G2 membranes showed improved rejection as the dendrimer loading increased, while G3 membranes showed maxima rejection at 99.8% at a dendrimer loading as low as the 0.71 μg/cm^2. Figure 8b,c shows the improvement for the modified membranes on salt rejection. With a 7.1 μg/cm^2 dendrimer deposition, both NaCl and $BaCl_2$ could be rejected to about 90%, which is not common for a low pressure NF membrane. Interestingly, membranes modified with dendrimer G2 showed a higher rejection to NaCl than those prepared with G3, while the opposite trend was found for the $BaCl_2$ rejection. Finally, the rejection of arsenic(III) by the membrane with either G2 or G3 modification was not as significantly increased at the lowest modification level (0.71 μg/cm^2), each of which increased from ca. 20% to 30%.

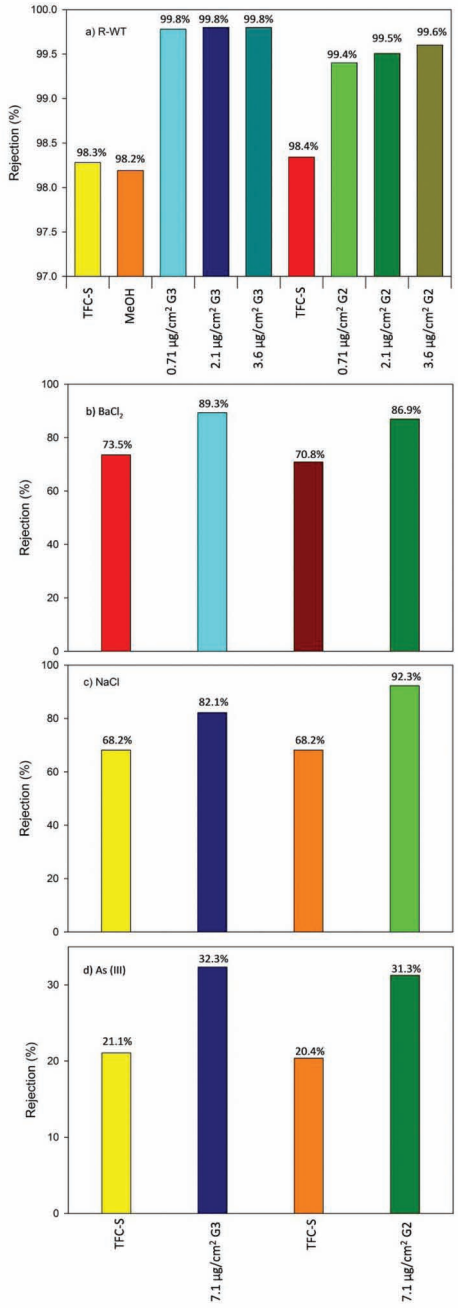

Figure 8. Rejection of prototypical contaminants by G2 or G3 modified TFC-S membranes. All data were acquired at a permeate flux of 0.4 m/day.

3. Conclusion

Our present research effort focused on utilizing shape-persistent dendritic architectures to modify a commercial nanofiltration (NF) membrane. Amphiphilic aromatic polyamide dendrimers (G1–G3) have been synthesized via a divergent approach and used for NF membrane modification by direct percolation. A PES-PVA film as control membrane and a commercial TFC-S NF membrane were used showing that structural compatibility between dendrimer and support plays an important role in the membrane modification process. All dendrimers broke through the PES-PVA UF support due to their hydrophilicity; however, they all formed additional coating on top of the TFC-S NF membrane in varying thickness with active layer properties. The dendrimer size had determinative effects in the formation of the new active layer, as increasing the dendrimer generation resulted in changes of percolation behavior, such as breakthrough of dendrimers and decrease in percolation flux. The membrane structures were further investigated by Rutherford backscattering spectrometry and AFM techniques, suggesting a

double active layer structure for the dendrimer-modified TFC-S membranes. Membrane performance was evaluated on the basis of rejection abilities of a variety of water contaminants and surrogates having a range of sizes and chemistry. The amount of deposited dendrimers was optimized to improve the solute rejection while minimizing water flux losses. The next research phase will focus on stabilizing the dendrimers on the support.

4. Experimental Section

Typical Procedure for Synthesis of NH_2-Terminated Aramide Dendrimer: *p*-Phenylene-diamine (54.1 mg, 0.50 mmol) was dissolved in NMP (1 mL). 3,5-Bis(trifluoroacetamido)benzoyl chloride (398.9 mg, 1.10 mmol) was added to this solution at 0 °C under nitrogen. The solution was stirred at the same temperature for 5 min, followed by 25 °C for 1 h. Water (0.1 mL) was then added and the solution was heated at 50 °C for 1 h. The reaction mixture was treated with hydrazine monohydrate (600 mg, 6.00 mmol) for 2 h at the same temperature and then poured into 2% $NaHCO_3$ solution (50 mL). The resultant white precipitate was filtered, washed with water, and dried at 120 °C under vacuum to give NH_2-G1 dendrimer as a white solid (178.8 mg, 95% yield). ^{1}H NMR (500 MHz, DMSO-d_6, δ): 9.87 (s, 2H, NH), 7.64 (s, 4H, Ar H), 6.27 (d, J = 1.5 Hz, 4H; Ar H), 5.97 (s, 2H, Ar H), 4.93 (s, 8H, NH_2); ^{13}C NMR (125 MHz, DMSO-d_6, δ): 166.7, 148.8, 136.7, 134.8, 120.1, 102.3 ppm.

Typical Procedure for Synthesis of Aramide Dendrimer with an OEG Periphery: NH_2-G1 dendrimer (23.1 mg, 0.06 mmol) was dissolved in NMP (2 mL). 2-[2-(2-Methoxyethoxy)ethoxy]acetyl chloride (72.4 mg, 0.37 mmol) was added to this solution at 0 °C under nitrogen. The solution was stirred at the same temperature for 5 min, followed by 25 °C for overnight. The reaction mixture was poured into 2% $NaHCO_3$ solution (20 mL) and extracted with CH_2Cl_2. The organic phase was washed with water, dried over anhydrous Na_2SO_4, and concentrated in vacuo. The residue solution was then placed on a Kugelrohr apparatus to remove remaining NMP solvent. The crude product was purified by column chromatography (CH_2Cl_2/MeOH, 15/1, v/v) to afford G1 as a light brown solid (62.3 mg, 84% yield). ^{1}H NMR (500 MHz, DMSO-d_6, δ): 10.29 (s, 2H, NH), 9.84 (s, 2H, NH), 8.24 (s, 2H, Ar H), 7.81 (d, J = 1.5 Hz, 4H; Ar H), 7.71 (s, 4H, Ar H), 4.10 (s, 8H, CH_2), 3.66-3.68 (m, 8H, CH_2), 3.60-3.61 (m, 8H, CH_2), 3.56-3.57 (m, 8H, CH_2), 3.44-3.46 (m, 8H, CH_2), 3.21 (s, 12H, CH_3); ^{13}C NMR (125 MHz, DMSO-d_6, δ): 171.2, 167.8, 139.6, 137.7, 136.3, 122.3, 116.7, 72.8, 72.0, 71.4, 71.3, 71.2, 59.1 ppm; MALDI-MS (dithranol, m/z): $[M]^+$ calcd 1016.5, found 1017.0; $[M+Na]^+$ calcd 1039.5, found 1039.0. GPC: 1800 (M_n), 1.03 (M_w/M_n).

Aramide Dendrimer Modification: All membranes were modified and tested using a bench-scale dead-end membrane filtration system (M8400, Millipore Co, Bedford, MA). Circular coupons of support membrane (PES-PVA or TFC-S) were cut and installed in such filtration reactor. The transmembrane pressure was set at 0.41 MPa (60 psi). The modified active layers were prepared by filtering methanol solutions containing approximately 6 mg/L of each aramide dendrimer (G1–G3) through the above support film at room temperature. The target mass of dendrimers loaded on TFC-S support was 1 mg. WINWEDGE software (TAL Technologies Inc., Philadelphia, PA) was used for real-time data collection of permeate flux of the methanol solution, which was measured gravimetrically with an analytical balance (BP211S, Sartorius Co., Edgewood, NY) connected to a computer. The amounts of dendrimers in permeate samples over time were monitored using a UV-visible spectrophotometer (UV-2401 PC, Shimadzu, Japan).

Membrane Characterization: Membranes modified with iodinated aramide dendrimers using either PES-PVA or TFC-S supports were characterized by RBS. The double active layer structured NF membranes based on the TFC-S support were further characterized by AFM.

RBS analysis were performed at room temperature with a 2-MeV He^+ beam generated by a Van de Graff accelerator. The incident, scattering and exit angles of the beam were 22.5°, 52.5°, and 150° respectively; the beam current was ca. 80 nA, and the beam diameter was 3 mm. The sample was scanned with the ion beam to limit the fluence of He^+ ions on the sample surface to a threshold value of 3×10^{14} He^+/cm^2. The RBS detector resolution was measured by testing a standard sample (5-Å-thick gold film, and 2 nm copper atop a layer of silicon). RBS data analyses were carried out with SIMNRA software.

Membranes were examined using an atomic force microscope (model Dimension 3100, Digital Instruments/Veeco). The instrument was operated in a tapping mode using silicon tips with nanometer scale resolution in air. The tip used for surface roughness analysis had a radius of 10 nm (BS-Tap300, Al coating, Nanoscience Instruments). For detection of ultrafine features, a 2-nm tip was used. Wet samples were dried at room temperature overnight and prior to testing. AFM images were obtained for the commercial TFC-S membrane and TFC-S membrane modified with dendrimers (G1–G3).

Membrane Performance Analysis: The performance of control and dendrimer-modified NF membranes was evaluated by measuring their rejection of R-WT, NaCl, $BaCl_2$, and As(III) at a constant permeate flux of 0.4 m/day at room temperature. Feed solutions of R-WT were prepared by dissolving this organic molecule in DDI to a concentration of 2.5 mg/L and adjusting the pH to 7.5. Feed solutions of NaCl and $BaCl_2$ were prepared by dissolving each salt in DDI to a concentration of 400 mg/L. Feed solutions of As(III) were prepared by dissolving $NaAsO_2$ (99% purity, Sigma-Aldrich) in DDI water. The pH was adjusted to 6 to ensure that all the arsenic was in the neutral arsenious acid (H_3AsO_3) form. The feed solution concentration was 4 mg/L as As. Magnetic stirring was used for minimizing solute concentration polarization during rejection testing. The concentration of R-WT in the feed and product water was measured by fluorescence (excitation/emission wavelengths 550/580 nm). Arsenious acid was analyzed by a colorimetric method using a UV-vis spectrophotometer (UV-2401PC, Shimadzu, Japan). The concentration of NaCl and $BaCl_2$ in feed and permeate samples was analyzed by ion chromatography (Dionex IC S-2000; Dionex ion Pac As 18 column, 36 mM KOH as eluent, 1 mL/min eluent flow rate, 25 mL injection loop). Solute rejection was calculated with the expression $SR = (1-c_p/c_f) \times 100\%$ where c_f and c_p are the solute concentrations in the feed and product water, respectively. The rejection performance data were analyzed by parameter fitting method using MATLAB software.

Supporting Information

Supporting Information is available from the Wiley Online Library or from the author.

Acknowledgements

This research has been partially supported by the Center for Microanalysis with funding from the U.S. Department of Energy under grant DEFG02-91-ER45439, and by the WaterCAMPWS, a Science and Technology Center of Advanced Materials for the Purification of Water with Systems under agreement number CTS-0120978. We also thank the Frederick Seitz Materials Research Laboratory Central Facilities, at the University of Illinois, which is partially supported by the U.S. Department of Energy under grant DEFG02-91-ER45439, and in particular Doug Jeffers and Scott McLaren.

Received: April 9, 2012
Revised: July 16, 2012
Published online: September 21, 2012

[1] a) T. Hillie, M. Hlophe, *Nat. Nanotechnol.* **2007**, *2*, 663; b) M. A. Shannon, P. W. Bohn, M. Elimelech, J. G. Georgiadis, B. J. Mariñas, A. M. Mayes, *Nature* **2008**, *452*, 301; c) M. A. Shannon, R. Semiat, *MRS Bull.* **2008**, *33*, 9.

[2] R. W. Baker, *Membrane Technology and Applications*, 2nd Ed., John Wiley and Sons, New York **2004**.
[3] B. X. Mi, O. Coronell, B. J. Mariñas, F. Watanabe, D. G. Cahill, I. Petrov, *J. Membr. Sci.* **2006**, *282*, 71.
[4] a) R. J. Petersen, *J. Membr. Sci.* **1993**, *83*, 81; b) R. Oizerovich-Honig, V. Raim, S. Srebnik, *Langmuir* **2010**, *26*, 299; c) J. Schaep, C. Vandecasteele, *J. Membr. Sci.* **2001**, *188*, 129.
[5] a) M. Elimelech, X. H. Zhu, A. E. Childress, S. K. Hong, *J. Membr. Sci.* **1997**, *127*, 101; b) E. M. Vrijenhoek, S. Hong, M. Elimelech, *J. Membr. Sci.* **2001**, *188*, 115; c) P. Xu, J. E. Drewes, T. U. Kim, C. Bellona, G. Amy, *J. Membr. Sci.* **2006**, *279*, 165.
[6] For rejection to salts, see: a) J. M. M. Peeters, J. P. Boom, M. H. V. Mulder, H. Strathmann, *J. Membr. Sci.* **1998**, *145*, 199; b) J. Schaep, B. Van der Bruggen, C. Vandecasteele, D. Wilms, *Sep. Purif. Technol.* **1998**, *14*, 155; for rejection to arsenic(III), see: c) Y. Sato, M. Kang, T. Kamei, Y. Magara, *Water Res.* **2002**, *36*, 3371; d) E. M. Vrijenhoek, J. J. Waypa, *Desalination* **2000**, *130*, 265.
[7] a) K. C. Khulbe, C. Feng, T. Matsuura, *J. Appl. Polym. Sci.* **2010**, *115*, 855; b) D. Li, H. T. Wang, *J. Mater. Chem.* **2010**, *20*, 4551.
[8] a) G. D. Kang, M. Liu, B. Lin, Y. M. Cao, Q. Yuan, *Polymer* **2007**, *48*, 1165; b) X. Y. Wei, Z. Wang, J. Chen, J. X. Wang, S. C. Wang, *J. Membr. Sci.* **2010**, *346*, 152.
[9] a) Y. Zhou, S. Yu, C. Gao, X. Feng, *Sep. Purif. Technol.* **2009**, *66*, 287; b) J. S. Louie, I. Pinnau, I. Ciobanu, K. P. Ishida, A. Ng, M. Reinhard, *J. Membr. Sci.* **2006**, *280*, 762.
[10] Y. Y. Lu, T. Suzuki, W. Zhang, J. S. Moore, B. J. Mariñas, *Chem. Mater.* **2007**, *19*, 3194.
[11] T. Suzuki, Y. Y. Lu, W. Zhang, J. S. Moore, B. J. Mariñas, *Environ. Sci. Technol.* **2007**, *41*, 6246.
[12] K. Kosutic, D. Dolar, B. Kunst, *J. Membr. Sci.* **2006**, *282*, 109.
[13] D. Astruc, E. Boisselier, C. Ornelas, *Chem. Rev.* **2010**, *110*, 1857.
[14] a) M. Jikei, M. A. Kakimoto, *J. Polym. Sci., Part A: Polym. Chem.* **2004**, *42*, 1293; b) M. Scholl, Z. Kadlecova, H. A. Klok, *Prog. Polym. Sci.* **2009**, *34*, 24.
[15] I. Washio, Y. Shibasaki, M. Ueda, *Org. Lett.* **2007**, *9*, 1363.
[16] K. Endo, Y. Ito, T. Higashihara, M. Ueda, *Eur. Polym. J.* **2009**, *45*, 1994.
[17] Q. Zhou, L. N. Zhang, H. Okamura, M. Minoda, T. Miyamoto, *J. Polym. Sci., Part A: Polym. Chem.* **2001**, *39*, 376.
[18] G. Schwarzenbacher, B. Evers, I. Schneider, A. de Raadt, J. Besenhard, R. Saf, *J. Mater. Chem.* **2002**, *12*, 534.
[19] A. V. R. Reddy, D. J. Mohan, A. Bhattacharya, V. J. Shah, P. K. Ghosh, *J. Membr. Sci.* **2003**, *214*, 211.
[20] D. M. Chao, X. B. Ma, X. F. Lu, L. L. Cui, H. Mao, W. J. Zhang, Y. Wei, *Macromol. Chem. Phys.* **2007**, *208*, 658.
[21] http://home.rzg.mpg.de/~mam/(last accessed September 2012)
[22] TFC-S membrane is composed of a polysulfone (PS) support and a polyamide thin layer of approximately 85 nm.
[23] P. Xu, J. E. Drewes, *Sep. Purif. Technol.* **2006**, *52*, 67.
[24] a) N. Vasanthan, D. R. Salem, *Mater. Res. Innovations* **2001**, *4*, 155; b) X. J. Zhang, D. G. Cahill, O. Coronell, B. J. Marinas, *J. Membr. Sci.* **2009**, *331*, 143.
[25] W. R. Bowen, T. A. Doneva, *Desalination* **2000**, *129*, 163.
[26] A. M. Saenz de Jubera, Y. Gao, J. S. Moore, D. Cahill, B. J. Marinas, *Environ. Sci. Technol.* **2012**, *46*, 9592.